Internal-quantum-state engineering using magnetic fields

Article (Published Version)

Internal-quantum-state engineering using magnetic fields

R. T. Sang, G. S. Summy,* B. T. H. Varcoe,† W. R. MacGillivray, and M. C. Standage
Laser Atomic Physics Laboratory, School of Science, Griffith University, Queensland, Nathan, 4111, Australia
(Received 28 August 2000; published 16 January 2001)

We present a general, semi-classical theory describing the interaction of an atom with an internal state consisting of a number of degenerate energy levels with static and oscillating magnetic fields. This general theory is applied to the $^3P_2$ metastable energy level of neon to determine the dynamics of the populations and coherences that are formed due to the interaction. Through these calculations we demonstrate how the interaction may be used for the internal state preparation of an atom.

DOI: 10.1103/PhysRevA.63.023408 PACS number(s): 42.50.Vk, 32.30.Bv

I. INTRODUCTION

The creation of state prepared atomic beams has a great number of applications in atomic physics research. For example, recent applications include cavity quantum electrodynamics [1], atom interferometers [2], and quantum computing [3]. In many cases this state preparation has been accomplished by optical pumping techniques via the application of resonant or near resonant light fields [4]. However, in many applications, this may not be the most appropriate technique to apply due to experimental constraints. For example the creation of well-defined populations and coherences of atoms within atom traps by laser interaction may lead to heating and can ultimately destroy the trapping conditions of the atoms. In some cases, the states of interest are metastable states and are not physically assessable via single-photon electric dipole allowed transitions.

Radio frequency (rf) spectroscopy has been a useful technique to investigate properties of neutral atoms since the pioneering experiments of Rabi [5]. The continued development of these techniques has had far reaching outcomes such as the definition of the second which is based on the probing of a rf ground state transition in Cs [6,7].

In the past five years there has been a great deal of interest in the application of magnetic traps for atoms to create weakly interacting gaseous Bose–Einstein condensates (BEC) [8]. The rf magnetic fields play an important role in the evaporative cooling process in the formation of BEC's [9,10]. By varying the frequency of the magnetic rf field, higher energy atoms can be removed from the trap by inducing transitions which place the selected atoms in atomic states which are not trapped, resulting in a decreased temperature for the remaining trapped atoms. A cw atom laser has been created via the application of rf fields to a trapped BEC [11]. In this case the rf field acts as an output coupler for atoms in the condensate by changing the state of atoms in a selected region of the trap to an untrapped state. The rf field determines the spatial extent to which atoms are ejected from the trap and the velocity of the atoms. It was also demonstrated that the BEC in this experiment could be manipulated on a micrometer scale with rf fields.

rf spectroscopy has also been applied to such trapped neutral atoms to determine their energy distribution [12,13]. Because of the very shallow trapping potential of such atoms, it is experimentally difficult to prepare them in specific atomic states using optical transitions due to the relatively large momentum transfer they experience in the absorption of a photon. Hence alternate state preparation techniques would be useful in this rapidly expanding field.

In this article we present a semi-classical theoretical analysis based on the Heisenberg equation of motion of the interaction of an atom with a static and rf magnetic field. This general theory is then applied to a specific example that is of interest to the authors through the development of an apparatus that will trap neon atoms in the $^2P_{3/2}3s[\frac{3}{2}]_2$ metastable state. We demonstrate how the technique can be used to produce an atomic state which has well-defined populations and coherences.

II. THEORY

Consider the interaction of both a weak static and an oscillating magnetic field on an ensemble of atoms with an arbitrary atomic state that is LS coupled with $J>0$. In the weak magnetic field limit, that is, the precession of the magnetic moment μ about J is much faster than that of J about the static magnetic field, the static magnetic field lifts the energy degeneracy of the magnetic sublevels m_J. The substate energy splittings are given by

$$\Delta E_{m_J} = g_J \mu_B B_{\text{Static}} m_J, \tag{1}$$

where μ_B is the Bohr magneton, B_{Static} is the magnitude of the static magnetic field, and g_J is the Landé g factor given by

$$g_J = 1 + \frac{j(j+1)+s(s+1)-l(l+1)}{2j(j+1)}, \tag{2}$$

where s and l are the spin and orbital angular momentum quantum numbers, respectively. Let B_{Static} be aligned with the z axis which is chosen as the quantization axis. A rf field of frequency ω_0 in the x-y plane,

*Clarendon Laboratory, Department of Physics, University of Oxford, Parks Road, Oxford OX1 3PU, United Kingdom.
†Max-Planck-Institute für Quantenoptik, Hans-Kopfermann Str 1, D-85748, Garching bei München, Germany.

$$\hat{B}(t)=\hat{B}_0[\cos\omega_0 t)\mathbf{i}+\sin(\omega_0 t)\mathbf{j}], \tag{3}$$

is also applied to the ensemble of atoms, where **i** and **j** are unit vectors in the *x* and *y* directions, respectively. The interaction of the atom with the time-varying magnetic field yields the interaction Hamiltonian:

$$\hat{H}_I=-\hat{\boldsymbol{\mu}}\cdot\hat{\mathbf{B}}(t), \tag{4}$$

where $\boldsymbol{\mu}$ is the magnetic dipole moment of the atom and is given by

$$\hat{\boldsymbol{\mu}}=-\frac{g_J\mu_B\hat{J}}{\hbar}. \tag{5}$$

To facilitate further simplification, the following operators are defined:

$$\hat{\boldsymbol{\mu}}_{\pm}=\hat{\mu}_x\mathbf{i}\pm i\hat{\mu}_y\mathbf{j}, \tag{6}$$

$$\hat{\mathbf{B}}_{\pm}=\hat{B}_x\mathbf{i}\pm i\hat{B}_y\mathbf{j}=\hat{B}_0e^{\pm i\omega_0 t}. \tag{7}$$

x

Hence from Eq. (5) it follows that the dipole operators can be written as

$$\hat{\boldsymbol{\mu}}_+=-\frac{g_J\mu_B\hat{\mathbf{J}}_+}{\hbar},\qquad \hat{\boldsymbol{\mu}}_-=-\frac{g_J\mu_B\hat{\mathbf{J}}_-}{\hbar}, \tag{8}$$

where $\hat{\mathbf{J}}_{\pm}$ are angular momentum operators defined in Cartesian coordinates as

$$\hat{\mathbf{J}}_{\pm}=\hat{J}_x\mathbf{i}\pm i\hat{J}_y\mathbf{j}. \tag{9}$$

These operators act as raising and lowering operators which connect states of different angular momenta and have eigenvalues that are given by

$$\hat{J}_+|j,m\rangle=\sqrt{j(j+1)-m(m+1)}\hbar|j,m+1\rangle,$$
$$\hat{J}_-|j,m\rangle=\sqrt{j(j+1)-m(m-1)}\hbar|j,m-1\rangle. \tag{10}$$

For simplicity, the vector notation has been dropped. The nonzero matrix elements of these operators are given by

$$\langle j,m\pm1|\hat{J}_{\pm}|j',m'\rangle=\sqrt{j'(j'+1)-m'(m'\pm1)}\hbar\,\delta_{jj'}\delta_{mm'}. \tag{11}$$

Therefore the matrix elements of the magnetic dipole operator may be written as

$$\mu_{gg'}=\frac{g_J\mu_B}{2\hbar}\left\langle g\left|\frac{\hat{J}_+}{\hbar}\right|g'\right\rangle=\frac{g_J\mu_B}{2\hbar}\left\langle g'\left|\frac{\hat{J}_-}{\hbar}\right|g\right\rangle, \tag{12}$$

where g and g' are dummy variables which represent the atomic basis states. Returning to the interaction Hamiltonian and, applying Eqs. (6) and (7) to Eq. (4) reveals

$$\hat{H}_I=-\tfrac{1}{2}(\hat{\mu}_+\hat{B}_-+\hat{\mu}_-\hat{B}_+). \tag{13}$$

This expression is now expanded over the orthonormal basis formed by the manifold of magnetic substates $|g\rangle$ of a particular fine structure level *J*:

$$\hat{H}_I=-\frac{1}{2}\sum_g\sum_{g'}\{|g\rangle\langle g|\hat{\mu}_+|g'\rangle\langle g'|\hat{B}_- +|g\rangle\langle g|\hat{\mu}_-|g'\rangle\langle g'|\hat{B}_+\}. \tag{14}$$

Defining atomic operators such that

$$\hat{\sigma}_{ij}=|i\rangle\langle j|, \tag{15}$$

where the states $\langle i|$ and $\langle j|$ are orthonormal atomic states, Eq. (14) can now be written as

$$\hat{H}_I=-\frac{1}{2}\sum_g\sum_{g'}\{\langle g|\hat{\mu}_+|g'\rangle\hat{B}_-+\langle g|\hat{\mu}_-|g'\rangle\hat{B}_+\}\hat{\sigma}_{gg'}. \tag{16}$$

Equation (16) can be expanded by dividing the sum over the basis states into two distinct regimes of dummy indices:

$$\hat{H}_I=-\frac{1}{2}\sum_{g>g'}\langle g|\hat{\mu}_+|g'\rangle\hat{B}_-\hat{\sigma}_{gg'} -\frac{1}{2}\sum_{g<g'}\langle g|\hat{\mu}_+|g'\rangle\hat{B}_-\hat{\sigma}_{gg'} -\frac{1}{2}\sum_{g>g'}\langle g|\hat{\mu}_-|g'\rangle\hat{B}_+\hat{\sigma}_{gg'} -\frac{1}{2}\sum_{g<g'}\langle g|\hat{\mu}_-|g'\rangle\hat{B}_+\hat{\sigma}_{gg'}. \tag{17}$$

The conditional operators within the summation signs run over the m_J substates and the condition that $g>g'$ is interpreted as the m_J value of $|g\rangle$ must be greater than the m_J value of $|g'\rangle$. Employing the raising and lowering properties of the dipole operator reduces Eq. (17) to

$$\hat{H}_I=-\frac{1}{2}\sum_{g>g'}\langle g|\hat{\mu}_+|g'\rangle\hat{B}_-\hat{\sigma}_{gg'} -\frac{1}{2}\sum_{g<g'}\langle g|\hat{\mu}_-|g'\rangle\hat{B}_+\hat{\sigma}_{gg'}. \tag{18}$$

Swapping the dummy indices of the second term allows for the expression to be placed under one summation sign, and applying Eqs. (7), (8), and (12) to this expression reveals

$$\hat{H}_I=\hbar\sum_{g>g'}\mu_{gg'}B_0e^{i\omega_0 t}\hat{\sigma}_{gg'}+\mu_{g'g}B_0e^{-i\omega_0 t}\hat{\sigma}_{g'g}, \tag{19}$$

where the operator notation for the oscillating magnetic field has been dropped since it commutes with the atomic operator at all times.

The atomic Hamiltonian is given by

$$\hat{H}_A = \hbar \sum_g \omega_g \hat{\sigma}_{gg}. \tag{20}$$

Thus the system Hamiltonian is

$$\hat{H} = \hbar \sum_g \omega_g \hat{\sigma} + \hbar \times \sum_{g>g'} (\mu_{gg'} B_0 e^{i\omega_0 t} \hat{\sigma}_{gg'} + \mu_{g'g} B_0 e^{-i_0 t} \hat{\sigma}_{g'g}). \tag{21}$$

In a technique analogous to that of Allen and Eberly [14], equations of motion for the atomic operators are derived in the Heisenberg representation which defines the time evolution of an atomic operator

$$\frac{d\hat{O}}{dt} = -\frac{i}{\hbar}[\hat{O}, \hat{H}]. \tag{22}$$

The equations of motion for the atomic operators have been derived following the procedure described in Farrell *et al.* [15]. For the general case they are given by

$$\begin{aligned}\frac{d\hat{\sigma}_{m_1 m_2}}{dt} = &-i(\omega_{m_2} - \omega_{m_1})\hat{\sigma}_{m_1 m_2} - i \sum_{g>m_2} L_{g m_2} e^{i\omega_0 t} \hat{\sigma}_{m_1 g} \\ &- i \sum_{m_2>g'} L_{m_2 g'} e^{-i\omega_0 t} \hat{\sigma}_{m_1 g'} \\ &+ i \sum_{g>m_1} L_{g m_1} e^{-i\omega_0 t} \hat{\sigma}_{g m_2} \\ &+ i \sum_{m_1>g'} L_{m_1 g'} e^{i\omega_0 t} \hat{\sigma}_{g' m_2},\end{aligned} \tag{23}$$

where the half-Larmor frequency is given by

$$L_{m_1 m_2} = \mu_{m_1 m_2} B_0. \tag{24}$$

The operators $\hat{\sigma}_{m_1 m_2}$ are transformed to slowly varying operators $\hat{\chi}_{m_1 m_2}$ by making the transformation

$$\hat{\chi}_{m_1 m_2} = \hat{\sigma}_{m_1 m_2} e^{i[m_2 - m_1]\omega_0 t}. \tag{25}$$

Substituting the slowly varying operators (25) into the equation of motion for the atomic operators (23) and taking expectation values yields

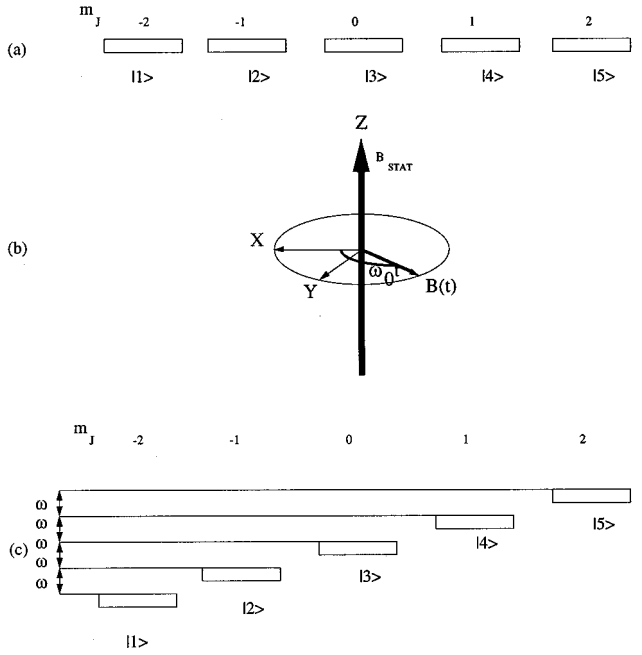

FIG. 1. The $^3P_2$ metastable state of neon. The states are degenerate without the application of a static magnetic field (a). (b) shows the geometry of the magnetic fields and shown in (c) is the lifting of the degeneracy with the application of a static magnetic field.

$$\begin{aligned}\frac{d\langle\hat{\chi}_{m_1 m_2}\rangle}{dt} = &-i(\omega_{m_2} - \omega_{m_1} - [m_2 - m_1]\omega_0)\langle\hat{\chi}_{m_1 m_2}\rangle \\ &- i \sum_{g>m_2} L_{g m_2} \langle\hat{\chi}_{m_1 g}\rangle - i \sum_{m_2>g'} L_{m_2 g'} \langle\hat{\chi}_{m_1 g'}\rangle \\ &+ i \sum_{g>m_1} L_{g m_1} \langle\hat{\chi}_{g m_2}\rangle + i \sum_{m_1>g'} L_{m_1 g'} \langle\hat{\chi}_{g' m_2}\rangle.\end{aligned} \tag{26}$$

The first term describes the free evolution of the system and indicates that the system will evolve even in the presence of a static magnetic field alone. The other terms in the equation represent the driving of the system by the oscillating field. It is interesting to note that there are no damping terms, which indicates that there is no steady-state limit as is the case with optical dipole transitions [15].

III. THEORETICAL RESULTS FOR A $J=2$ STATE

As an example of the general theory derived above we now apply it to the $^2P_{3/2}3s[\frac{3}{2}]_2$ state of neon (written in the *JK* coupling scheme). This first excited state is metastable with a lifetime of 20 s and is well approximated by the *L*-*S* coupling scheme [16] such that *J* is a good quantum number. It will be denoted from here onwards as the $^3P_2$ $(J=2)$ state. This state has been the subject of many experimental investigations as a result of optical cooling and trapping of atoms in this state [17].

Figure 1(a) illustrates the $^3P_2$ magnetic projection substates prior to the interaction with the magnetic fields. Both

TABLE I. The nonzero matrix elements $\mu_{gg'}$ for the $^3P_2$ manifold which are defined by Eq. (12).

$\mu_{gg'}$	$\left\langle m_1 \left\vert \frac{\hat{J}_+}{\hbar} \right\vert m_2 \right\rangle \frac{g_J \mu_B}{2\hbar}$
μ_{21}	$2\frac{g_J \mu_B}{2\hbar}$
μ_{32}	$\sqrt{6}\frac{g_J \mu_B}{2\hbar}$
μ_{43}	$\sqrt{6}\frac{g_J \mu_B}{2\hbar}$
μ_{54}	$2\frac{g_J \mu_B}{2\hbar}$

the static and time-varying magnetic fields and their orientations are shown in Fig. 1(b). The quantization axis is chosen to be along the z axis which is the same as for the generalized theory derived in Sec. II. The effect of the fields on the state is depicted in Fig. 1(c). The selection rules for the allowed transitions between the basis states are defined by Eq. (12) and the nonzero matrix elements for this example are given in Table I written in terms of the constant factor $g_J \mu_B / 2\hbar = 6.626 \times 10^6\ \mathrm{G^{-1}\,s^{-1}}$.

Applying Eq. (26) to this system yields the equations of motion in the Appendix where the substate numbers defined in Fig. 1 have been applied. These equations define a set of coupled, linear, first-order differential equations the solutions of which can be found utilizing a number of algorithms (see for example [4]). These equations effectively describe a set of undamped, coupled harmonic oscillators. It is important to note that under certain conditions the entire system will not evolve at all. This occurs, for example, if all of the substate populations are identical and there are no coherences between them. In this case all of the terms on the rhs of the equations are zero, indicating that the system is static. Thus to observe any dynamics on this system an initial population difference must be created. This could be accomplished, for example, through optical pumping which is possible utilizing the $^2P_{3/2}3s[\frac{3}{2}]_2 \rightarrow {}^3P_{3/2}3s[\frac{5}{2}]_2$ transition. No population losses should occur in this case as the transition is completely closed.

The equations of motion defined in the Appendix also illustrate the possible ways of state preparing an atomic beam. Provided that there is a nonuniform initial population distribution prior to the interaction with the magnetic fields, then the populations and coherences in the $J=2$ state will evolve and will continue to do so in the presence of the fields. If the evolution is stopped by suddenly turning off these fields, then the atoms will remain with a particular population distribution and also maintain their coherences. This ''switch off'' could be achieved by varying the transit time of the interaction of the atoms with the fields or by varying the magnetic field strength or detuning for a fixed transit time of the atoms through the interaction region. The last two methods should be easier to achieve experimentally.

Figure 2 shows the populations and coherences as a function of time for zero detuning with two different oscillating field amplitudes. In the zero detuning case, the static magnetic field splits the substates by equal energy differences and the frequency ω_0 of the oscillatory field is chosen to match the transition frequency between each substate. Labels such as $|mn\rangle$ refer to the coherence formed between states $|m\rangle$ and $|n\rangle$. In Figs. 2(a)–(c) the amplitude of the oscillating field, $B(t)$ is 0.1 G, while in Figs. 2(d)–(f) the amplitude is 0.5 G. It has been assumed that at the start of the interaction only state $|1\rangle$ is populated.

Figure 2(a) shows the population as a function of time. The effect of the oscillating field is to pump the population from state $|1\rangle$ to state $|5\rangle$ and back again to state $|1\rangle$ then repeating this cycle. As a result of the equations of motion for the populations $|1\rangle$ and $|5\rangle$ depending on a single Larmor frequency, the period of the cycle for these populations is equal to the inverse of the L_{12}, L_{45} half Larmor frequencies (which are equal) defined by Eq. (24). In the absence of damping this trend would continue as long as the atoms are in the presence of the magnetic fields. In the case of the populations $|2\rangle$, $|3\rangle$ and $|4\rangle$ the cycling of the populations is more complex due to the interplay of different Larmor frequencies. Figure 2(d) shows the same general trend for the populations although the period of the population transfer is faster as expected for a driving field of larger amplitude. The coherences of the form $|m,m-1\rangle$ are associated with the absorption of a single rf photon. When the detuning is zero, these terms are imaginary as they are purely absorptive. $|21\rangle$, $|32\rangle$, $|43\rangle$ and $|54\rangle$ are coherences of this type and are plotted in Fig. 2(b). Their complex conjugates are identical in magnitude but opposite in sign and have not been plotted. These coherences are zero when the atoms have been pumped entirely to substate $|1\rangle$ or substate $|5\rangle$. When the atoms are being pumped ''up the energy ladder'' $|1\rangle$ to $|5\rangle$ [i.e., their internal energy is increased, see Fig. 1(c)] these coherences are positive, while they are negative on returning ''down the energy ladder'' from substate $|5\rangle$ to substate $|1\rangle$. These processes are analogous to stimulated absorption and stimulated emission in an electric dipole transition.

The coherence term $|41\rangle$ represents a three-photon process and the phase of this coherence is given by the sum of the phases of the $|43\rangle$, $|32\rangle$ and $|21\rangle$ coherences. Since these coherences were purely imaginary, this coherence will also be purely imaginary but will be opposite in sign to the single-photon coherences. A similar argument holds for the sign of the coherence $|52\rangle$.

The coherence terms plotted in Fig. 2(c) result from an even number of photon processes. For example, the relative phase of the coherence $|31\rangle$ is given by the sum of the phases of the coherences $|32\rangle$ and $|21\rangle$. Since these two coherences are purely imaginary, it follows that $|31\rangle$ must be real. A similar argument can be used for the coherences $|42\rangle$ and $|53\rangle$. The coherence $|51\rangle$ results from a four-photon process and as such will have a π phase difference (and subsequent sign change) with respect to the two-photon terms.

Figures 2(d)–(f) show the identical general trends as Figs. 2(a)–(c) but with shorter time scales owing to the increased

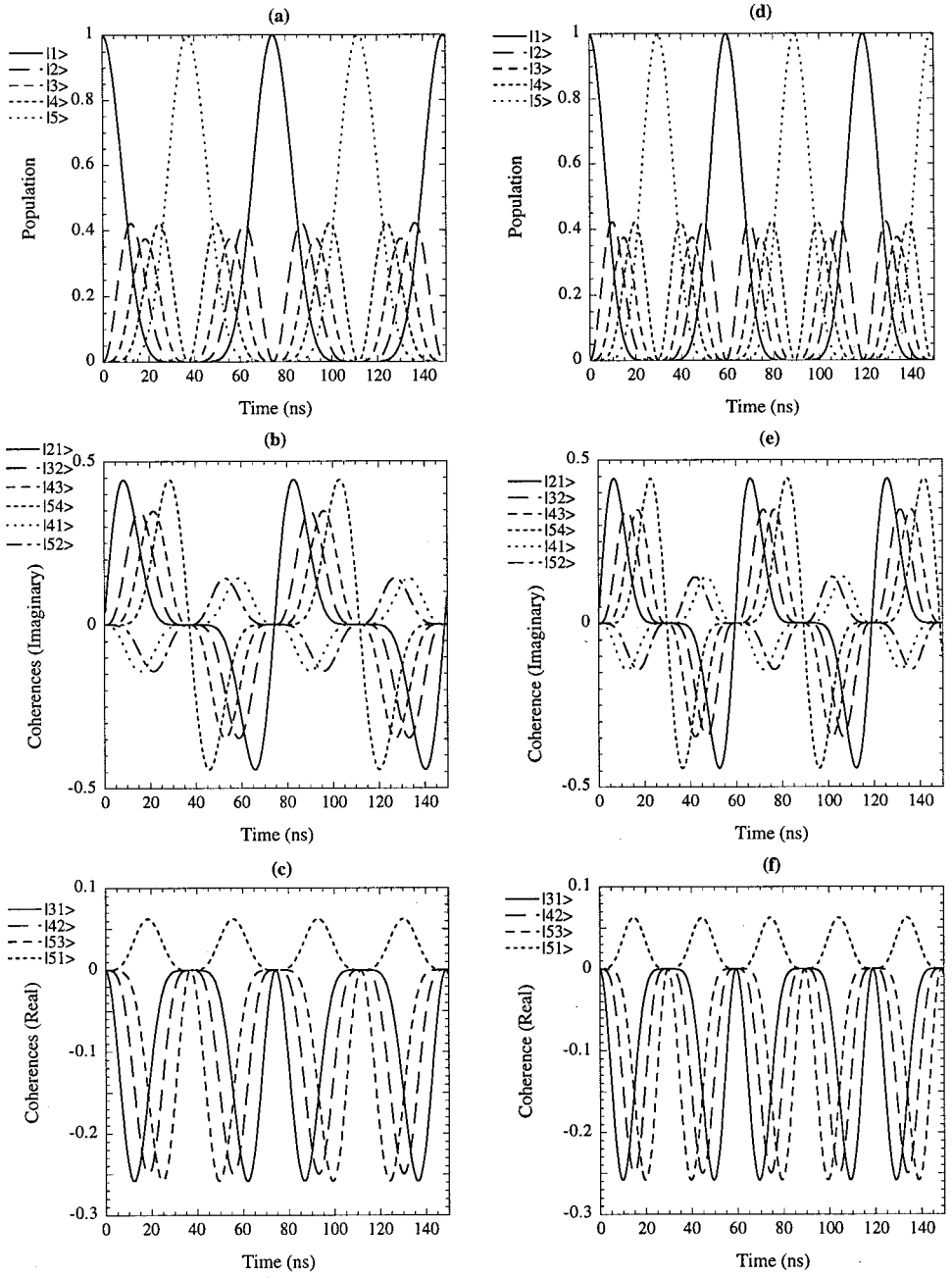

FIG. 2. Populations and coherences as a function of time. All figures are with zero detuning. Figures (a)–(c) have an oscillating field amplitude of 0.1 G and figures (d)–(f) have an oscillating field amplitude of 0.5 G.

Larmor frequency attributed to the larger amplitude of the oscillating magnetic field.

The graphs in Fig. 3 represent the populations and coherences as a function of the strength of the oscillating magnetic field for a range of 0–0.2 G at zero detuning. It has been assumed in the calculation that the atoms have a constant interaction time with the field of 10 μs which for a beam of neon atoms travelling at 900 m/s corresponds to an interaction region of approximately 0.9 cm. This constant interaction time is not realistic for a thermal beam of atoms since there would be a range of times due to the Maxwell–Boltzman distribution of longitudinal velocities. However, utilizing laser cooling and two-dimensional trapping schemes, the longitudinal velocity distributions can be greatly reduced. This type of state preparation could also be used for trapped or laser-cooled atoms where the small spread in atomic velocities would make it possible for all atoms to experience nearly the same time in the preparation region. The graphs display the same behavior as the time-dependent case in Fig. 2. This result is expected since, as shown in Fig. 2, changing of the amplitude of the oscillating field results in a change of the frequency at which the population cycles. Hence, varying the amplitude of the field results in a phase shift of the populations and coherences and constitutes another mechanism by which the population and coherences may be controlled. Since the detuning is zero, the

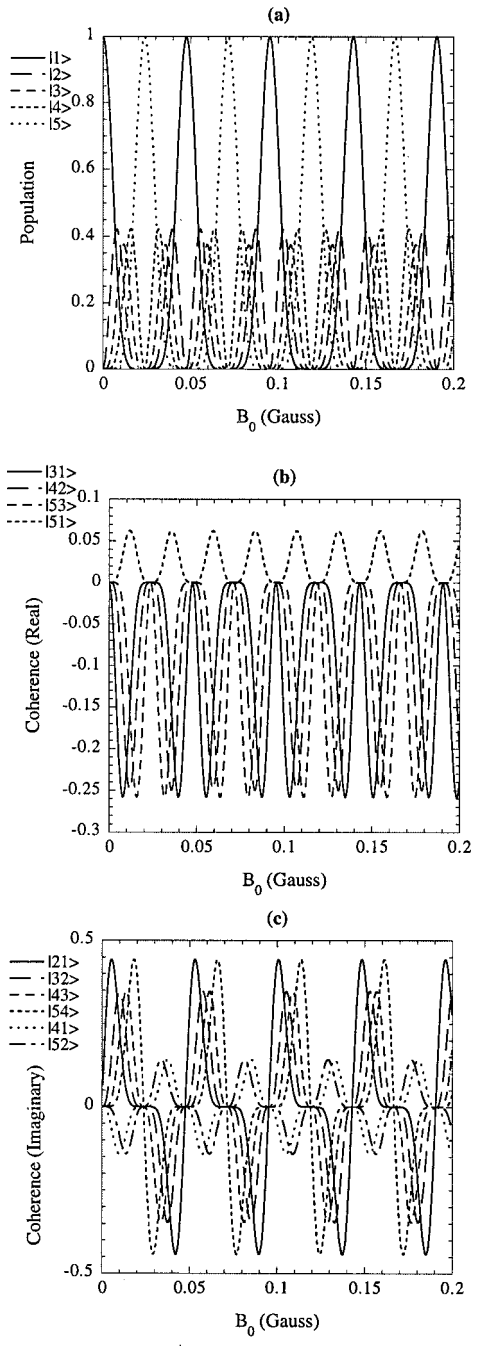

FIG. 3. Populations and coherences as a function of oscillating field amplitude for zero detuning and an interaction time of 10 μs.

same type of coherences that were formed in Fig. 2 must again be formed in Fig. 3.

Figure 4 shows the populations and coherences as a function of detuning of the oscillating field for a constant time of 10 μs and a constant magnetic field amplitude of 0.1 G. Figure 4(a) shows that the populations have a great deal of structure that is symmetric about zero detuning. The populations oscillate, with the amplitude of the oscillations decreasing as the detuning is increased. The general trend is that the population in state $|1\rangle$ increases while the populations in all other states decrease as the detuning is increased. The interpretation of this is that at large detunings there is only a small probability of excitation. As a result, if the population is initially in state $|1\rangle$, then only a small portion of the population will be transferred at large detuning.

The coherences formed are shown in the remaining graphs of Fig. 4. Over most of the detuning range, these terms are complex. The real parts of the coherences formed by an odd number of photon processes display antisymmetric ''dispersive''-type behavior about zero detuning, while their imaginary parts exhibit symmetric ''absorptive'' behavior. The opposite effect is demonstrated by coherences relating to an even number of photon processes which is consistent with their relative phases. At large detunings only the $|21\rangle$ and $|31\rangle$ terms are significant as the populations are not pumped beyond substate $|3\rangle$. All the coherences have repeated zero values at the detunings for which the atoms have been pumped entirely into substate $|1\rangle$.

IV. APPLICATIONS

In this article we have presented a general, semi-classical, theoretical analysis of atomic state preparation using magnetic fields. The general theory has been applied to a $J=2$ state of neon. A clear application of the technique outlined in this article is its application in the creation of user-defined populations and coherences in an atomic ensemble. The calculations in Sec. III have demonstrated three ways of achieving this. The first way would be to allow the atoms to interact with fields of well-defined amplitude and detuning for a specific length of time. For example, in Fig. 2(a), if the interaction time is set to approximately 38 ns, or multiples of that period, then the population is totally transferred to substates with the opposite sign $(-m_J)$. It is also interesting to observe that in the case of the coherences, there are points on the graph at which all coherences are nearly zero except for one. For example, in Fig. 2(c) at around 38 ns, the coherence $|54\rangle$ is much larger than any of the other coherences. This permits the ''engineering'' of an atomic ensemble in an atomic state with a single coherence. Figures 3 and 4 demonstrate that for well-defined interaction times, populations and coherences can be engineered for various oscillating magnetic field amplitudes and detunings. The easiest method to employ experimentally would be to maintain the interaction time and the detuning constant and vary the amplitude of the field so as to create the desired populations and coherences.

This type of state preparation technique has advantages for the application of laser-cooled or trapped atoms, since the momentum kick delivered by the rf photons is small compared to that of optical photons. As such it is possible to create well-defined populations and coherences without significantly heating the atoms. This would be ideal for internal state manipulation of Bose–Einstein condensates. It is also possible to ''tune'' this momentum kick since the wavelength of the rf photons depends on the splitting of the degenerate energy levels which is dependent on the applied static magnetic field.

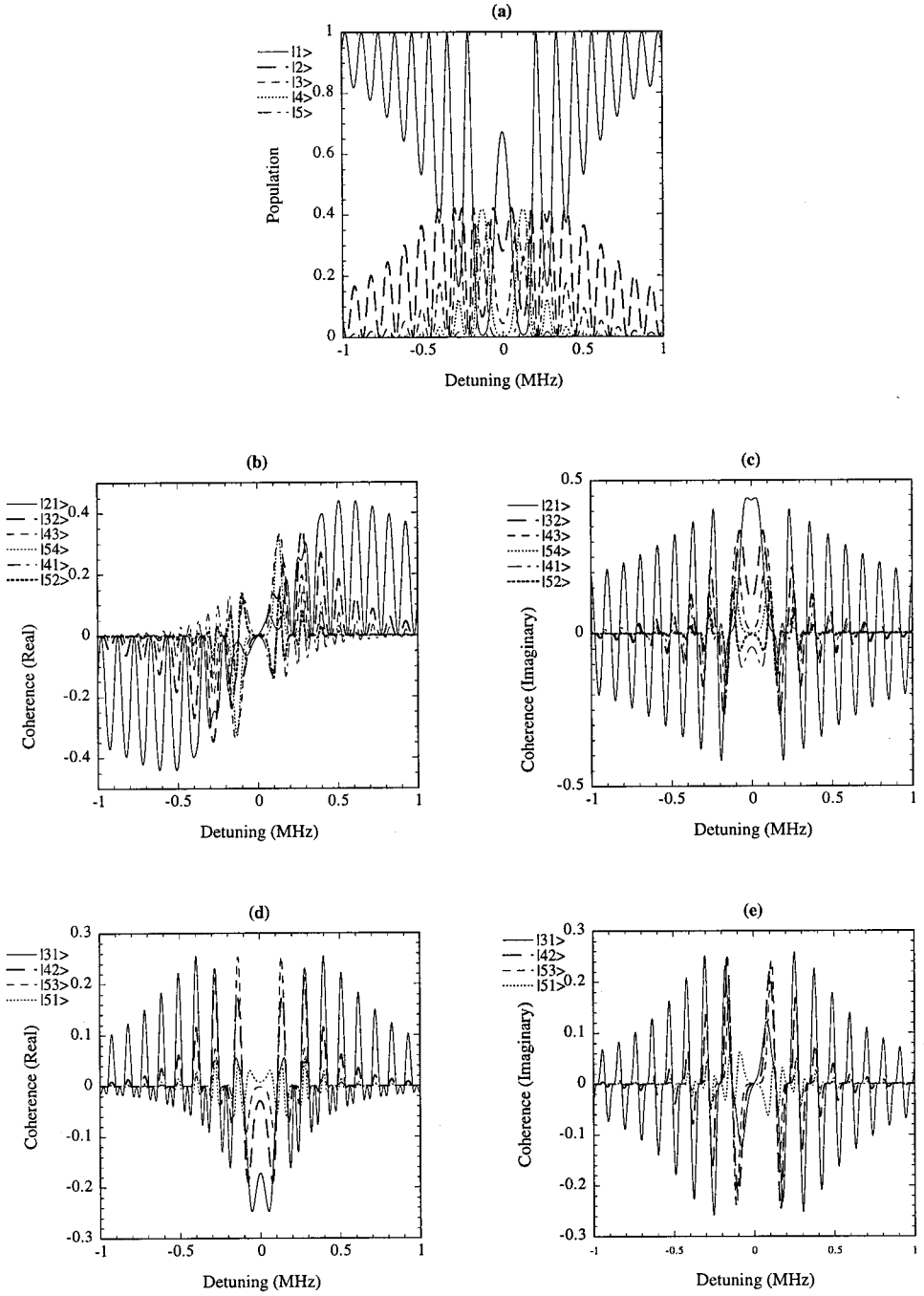

FIG. 4. Populations and coherences as a function of detuning the oscillating field for a constant oscillating field amplitude of 0.1 G and constant interaction time of 10 μs.

ACKNOWLEDGMENTS

All calculations were performed at the Queensland Parallel Super-computing facility at Griffith University. The authors would like to acknowledge the assistance of the Australian Research Council and the School of Science at Griffith University for funding aspects of the research. RTS was supported by an Australian Research Council Postdoctoral Fellowship Scheme.

APPENDIX

Populations:

$$\frac{d\langle\hat{\chi}_{11}\rangle}{dt} = -iL_{12}\langle\hat{\chi}_{12}\rangle + iL_{12}\langle\hat{\chi}_{21}\rangle, \tag{A1}$$

$$\frac{d\langle\hat{\chi}_{22}\rangle}{dt} = -iL_{12}\langle\hat{\chi}_{21}\rangle + iL_{12}\langle\hat{\chi}_{12}\rangle - iL_{23}\langle\hat{\chi}_{23}\rangle + iL_{23}\langle\hat{\chi}_{32}\rangle, \tag{A2}$$

$$\frac{d\langle\hat{\chi}_{33}\rangle}{dt} = -iL_{23}\langle\hat{\chi}_{32}\rangle + iL_{23}\langle\hat{\chi}_{23}\rangle - iL_{34}\langle\hat{\chi}_{34}\rangle + iL_{34}\langle\hat{\chi}_{43}\rangle, \tag{A3}$$

$$\frac{d\langle\hat{\chi}_{44}\rangle}{dt} = -iL_{34}\langle\hat{\chi}_{43}\rangle + iL_{34}\langle\hat{\chi}_{34}\rangle - iL_{45}\langle\hat{\chi}_{45}\rangle + iL_{45}\langle\hat{\chi}_{54}\rangle, \tag{A4}$$

$$\frac{d\langle\hat{\chi}_{55}\rangle}{dt} = -iL_{45}\langle\hat{\chi}_{54}\rangle + iL_{45}\langle\hat{\chi}_{45}\rangle. \tag{A5}$$

Coherences:

$$\frac{d\langle\hat{\chi}_{21}\rangle}{dt} = -i\Delta\langle\hat{\chi}_{21}\rangle + iL_{23}\langle\hat{\chi}_{31}\rangle + iL_{12}\langle\hat{\chi}_{11}\rangle - iL_{12}\langle\hat{\chi}_{22}\rangle, \tag{A6}$$

$$\frac{d\langle\hat{\chi}_{12}\rangle}{dt} = i\Delta\langle\hat{\chi}_{12}\rangle - iL_{23}\langle\hat{\chi}_{13}\rangle - iL_{12}\langle\hat{\chi}_{11}\rangle + iL_{12}\langle\hat{\chi}_{22}\rangle, \tag{A7}$$

$$\frac{d\langle\hat{\chi}_{32}\rangle}{dt} = -i\Delta\langle\hat{\chi}_{32}\rangle + iL_{34}\langle\hat{\chi}_{42}\rangle + iL_{23}\langle\hat{\chi}_{22}\rangle - iL_{23}\langle\hat{\chi}_{33}\rangle - iL_{12}\langle\hat{\chi}_{31}\rangle, \tag{A8}$$

$$\frac{d\langle\hat{\chi}_{23}\rangle}{dt} = i\Delta\langle\hat{\chi}_{23}\rangle - iL_{43}\langle\hat{\chi}_{24}\rangle - iL_{32}\langle\hat{\chi}_{22}\rangle + iL_{32}\langle\hat{\chi}_{33}\rangle + iL_{12}\langle\hat{\chi}_{13}\rangle, \tag{A9}$$

$$\frac{d\langle\hat{\chi}_{43}\rangle}{dt} = -i\Delta\langle\hat{\chi}_{43}\rangle - iL_{34}\langle\hat{\chi}_{44}\rangle - iL_{23}\langle\hat{\chi}_{42}\rangle + iL_{45}\langle\hat{\chi}_{53}\rangle + iL_{34}\langle\hat{\chi}_{33}\rangle, \tag{A10}$$

$$\frac{d\langle\hat{\chi}_{34}\rangle}{dt} = i\Delta\langle\hat{\chi}_{34}\rangle + iL_{34}\langle\hat{\chi}_{44}\rangle + iL_{23}\langle\hat{\chi}_{24}\rangle - iL_{45}\langle\hat{\chi}_{35}\rangle - iL_{34}\langle\hat{\chi}_{33}\rangle, \tag{A11}$$

$$\frac{d\langle\hat{\chi}_{54}\rangle}{dt} = -i\Delta\langle\hat{\chi}_{54}\rangle - iL_{45}\langle\hat{\chi}_{55}\rangle - iL_{34}\langle\hat{\chi}_{53}\rangle + iL_{45}\langle\hat{\chi}_{44}\rangle, \tag{A12}$$

$$\frac{d\langle\hat{\chi}_{45}\rangle}{dt} = i\Delta\langle\hat{\chi}_{45}\rangle + iL_{45}\langle\hat{\chi}_{55}\rangle + iL_{34}\langle\hat{\chi}_{35}\rangle - iL_{45}\langle\hat{\chi}_{44}\rangle, \tag{A13}$$

$$\frac{d\langle\hat{\chi}_{31}\rangle}{dt} = -2i\Delta\langle\hat{\chi}_{31}\rangle - iL_{12}\langle\hat{\chi}_{32}\rangle + iL_{34}\langle\hat{\chi}_{41}\rangle + iL_{23}\langle\hat{\chi}_{21}\rangle, \tag{A14}$$

$$\frac{d\langle\hat{\chi}_{13}\rangle}{dt} = 2i\Delta\langle\hat{\chi}_{13}\rangle + iL_{12}\langle\hat{\chi}_{23}\rangle - iL_{34}\langle\hat{\chi}_{14}\rangle - iL_{23}\langle\hat{\chi}_{12}\rangle, \tag{A15}$$

$$\frac{d\langle\hat{\chi}_{42}\rangle}{dt} = -2i\Delta\langle\hat{\chi}_{42}\rangle - iL_{23}\langle\hat{\chi}_{43}\rangle - iL_{12}\langle\hat{\chi}_{41}\rangle + iL_{34}\langle\hat{\chi}_{32}\rangle + iL_{45}\langle\hat{\chi}_{52}\rangle, \tag{A16}$$

$$\frac{d\langle\hat{\chi}_{24}\rangle}{dt} = 2i\Delta\langle\hat{\chi}_{24}\rangle + iL_{23}\langle\hat{\chi}_{34}\rangle + iL_{12}\langle\hat{\chi}_{14}\rangle - iL_{34}\langle\hat{\chi}_{23}\rangle - iL_{45}\langle\hat{\chi}_{25}\rangle, \tag{A17}$$

$$\frac{d\langle\hat{\chi}_{53}\rangle}{dt} = -2i\Delta\langle\hat{\chi}_{53}\rangle - iL_{34}\langle\hat{\chi}_{54}\rangle - iL_{23}\langle\hat{\chi}_{52}\rangle + iL_{45}\langle\hat{\chi}_{43}\rangle, \tag{A18}$$

$$\frac{d\langle\hat{\chi}_{35}\rangle}{dt} = 2i\Delta\langle\hat{\chi}_{35}\rangle + iL_{34}\langle\hat{\chi}_{45}\rangle + iL_{23}\langle\hat{\chi}_{25}\rangle - iL_{45}\langle\hat{\chi}_{34}\rangle, \tag{A19}$$

$$\frac{d\langle\hat{\chi}_{41}\rangle}{dt} = -3i\Delta\langle\hat{\chi}_{41}\rangle - iL_{12}\langle\hat{\chi}_{42}\rangle + iL_{45}\langle\hat{\chi}_{51}\rangle + iL_{34}\langle\hat{\chi}_{31}\rangle, \tag{A20}$$

$$\frac{d\langle\hat{\chi}_{14}\rangle}{dt} = 3i\Delta\langle\hat{\chi}_{14}\rangle + iL_{12}\langle\hat{\chi}_{24}\rangle - iL_{45}\langle\hat{\chi}_{15}\rangle - iL_{34}\langle\hat{\chi}_{13}\rangle, \tag{A21}$$

$$\frac{d\langle\hat{\chi}_{52}\rangle}{dt} = -3i\Delta\langle\hat{\chi}_{52}\rangle - iL_{23}\langle\hat{\chi}_{53}\rangle - iL_{12}\langle\hat{\chi}_{51}\rangle + iL_{45}\langle\hat{\chi}_{42}\rangle, \tag{A22}$$

$$\frac{d\langle\hat{\chi}_{25}\rangle}{dt} = 3i\Delta\langle\hat{\chi}_{25}\rangle + iL_{23}\langle\hat{\chi}_{35}\rangle + iL_{12}\langle\hat{\chi}_{15}\rangle - iL_{45}\langle\hat{\chi}_{24}\rangle, \tag{A23}$$

$$\frac{d\langle\hat{\chi}_{51}\rangle}{dt} = -4i\Delta\langle\hat{\chi}_{51}\rangle - iL_{12}\langle\hat{\chi}_{52}\rangle + iL_{45}\langle\hat{\chi}_{41}\rangle, \tag{A24}$$

$$\frac{d\langle\hat{\chi}_{15}\rangle}{dt} = 4i\Delta\langle\hat{\chi}_{15}\rangle + iL_{12}\langle\hat{\chi}_{25}\rangle - iL_{45}\langle\hat{\chi}_{14}\rangle, \tag{A25}$$

where Δ is the detuning between the oscillating field frequency and the frequency interval between the Zeeman sublevels.

[1] G. Raithel, C. Wagner, H. Walther, L. M. Narducci, and M. O. Scully, Adv. At. Mol. Phys. **Suppl. 2**, 57 (1994).

[2] C. S. Adams, M. Sigel, and J. Mlynek, Phys. Rep. **240**, 143 (1994).

[3] A. M. Steane, Rep. Prog. Phys. **61**, 117 (1998).

[4] B. T. H. Varcoe, R. T. Sang, W. R. MacGillivray, M. C. Standage, and P. M. Farrell, J. Mod. Opt. **46**, 787 (1999).

[5] I. I. Rabi, J. R. Zacharias, S. Millman, and P. Kusch, Phys. Rev. **53**, 318 (1938).

[6] N. F. Ramsey, Phys. Today **33**(7), 25 (1980).

[7] N. F. Ramsey, *Molecular Beams* (Oxford U. P., New York, 1956).
[8] H. J. Metcalf and P. van der Straten, *Laser Cooling and Trapping* (Springer, New York, 1999), pp. 241–250.
[9] M. H. Anderson, J. K. Ensher, M. R. Matthews, C. E. Wieman, and E. A. Cornell, Science **269**, 198 (1995).
[10] K. B. Davis, M.-O. Mews, M. R. Andrews, N. J. van Druten, D. S. Durfee, D. M. Kurn, and W. Ketterle, Phys. Rev. Lett. **75**, 3969 (1995).
[11] I. Bloch, T. Haensch, and T. Esslinger, Phys. Rev. Lett. **82**, 3008 (1999).
[12] A. Martin, K. Helmerson, V. Bagnato, G. Lafyatis, and D. Pritchard, Phys. Rev. Lett. **61**, 2431 (1988).
[13] K. Helmerson, A. Martin, and D. Pritchard, J. Opt. Soc. Am. B **9**, 483 (1992).
[14] L. Allen and J. H. Eberly, *Optical Resonance and Two Level Atoms* (Wiley, New York, 1975).
[15] P. M. Farrell, W. R. MacGillivray, and M. C. Standage, Phys. Rev. A **37**, 4240 (1988).
[16] M. A. Khakoo, T. Tran, D. Bordelon, and G. Csanak, Phys. Rev. A **45**, 219 (1992).
[17] F. Shimizu, K. Shimizu, and H. Takuma, Chem. Phys. **145**, 327 (1990).